Effect on the Local Seismic Response Produced by the Construction of Rafted Piles Foundation

Mirko Lago[1], Annalisa Trevisan[2], Francesco Veronese[3]

[1]*Freelance Professional, Rovigo Italy*
[2]*Freelance Professional, Cinto Euganeo (Pd) Italy*
[3]*Infrastrutture Venete, Rovigo Italy*
[#]*Corresponding author: trevisannalisa@gmail.com*

ABSTRACT

The seismic forces must be properly defined as required by European geotechnical design Codes. They are dependent from the morphological and stratigraphic characteristics that determine the local seismic response. The local seismic response can be evaluated using a simplified approach which is based on the classification of the subsoil according to the values of the shear wave propagation speed Vs. In the present case study, to complete the quay of the Rovigo Interporto (facing the River Canal Bianco), where a not negligible load is planned to be applied (50 kPa), has been designed a foundation with a large slab founded with not pre-casted reinforced concrete piles diameter 350 mm, drilled without removing soil, with vibrating casing, for settlement reduction (rafted piles as settlement reducers), on an area of approximately 6000 m^2. The subsoil in this area, from geological and geotechnical point of view, is very variable and with layers of soft clay and loose sand or silt, with no presence of a dense and uniform sand layer where to transfer loads to. Moreover, the geotechnical model was complicated because of the presence of an old diaphragm wall with anchors (whose projection in plant covers around half of area) and was designed a large underground basin for hydraulic invariance. For this reason, an extensive campaign of CPTU and DMT tests, together with boreholes, sampling and laboratory tests was carried out in this area, which allowed a detailed characterization of the subsoil. Through direct measurement of seismic micro-tremors, carried out before and after the installation of the piles, has been evaluated the modification of the resonance frequency of the site, and modification of the propagation speed of the shear waves Vs induced by the slab over rafted piles over the entire area.

Keywords: Borehole, CPTU, DMT, HVSR, Rafted piles, SCPTU, Seismic response

1. Description of the project

The internal Port of Rovigo, as identified by the Regional Transport Plan 2020-2030, is not only one of the five buildings structures that make up the Regional Interport System but is also a “unicum” in the Veneto System, because the three methods of transporting goods are concentrated: on road, on rail and by water. It is connected to the Mantua-Venice waterway, via a dedicated railway connection, joined to the Bologna-Padova railway line, and finally, on the road and motorway traffic via road connection.

The intervention includes the consolidation of area of approximately 6000 m^2 of the Rovigo internal port quay, currently unpaved and therefore unusable, through the construction of a pile-cap foundation. The piles are designed for reducing settlements and to assure a maximum homogeneous final bearing capacity of 50 kN/m^2. The scope of the project is to increase the development on the Interport from a commercial and the tourist point of view.

To comply with current legislation about the hydraulic system (DGR 2948/2009), the work also includes the construction of a reinforced concrete tank (dimension 35x18x1.40 m) to collect rainwater runoff from the pavement. Finally, the subgrade of the roads shall be suitable to guarantee heavy traffic.

With another procurement, on the same area, will be realized the electrification of the port quay (cold ironing), which will involve the implementation of the columns for electricity supply of the nautical units to stay on the quay and the support system on the quay area (lighting, fire prevention, electric, video surveillance, underground services in general).

The project area was divided into five zones (how to show in the figure 1), depending on type of works and expected project loads:

- ZONE 1: area where the structures serving "Cold-Ironing" are located: Light Tower, CE01 Cabin, Fire Tank and all related services
- ZONE 2: area where maximum project loads are 20 kN/m^2. The tie-rod are located only in a little portion of this area, furthermore in this area are located the hydraulic systems of the first rain tank that will bear only the loads of the handling vehicles.
- ZONE 3: area where the maximum loads are 50 kN/ m^2, in this area are located the tie rods.
- ZONE 4: a lamination tank is planned to comply with hydraulic invariance, measuring approximately 662 m^2. The tank must however be suitable to withstand a load of 50 kN/m^2 in addition to its own weight and the weight of the layers above. The structure of the tank in zone 4 is designed in such a way as not to interfere with the tie rods which, in that area, are present at depths greater than 7 metres.

• ZONE 5: the width of this area is approximately 3 m. It is delimitated by the diaphragm on the southwest northeast direction. The maximum loads are 50 kN/m^2 but will be made a cap foundation on piles 15 m long. The reinforced concrete cap foundation is 1m high and linked the existent quay diaphragm walls with the new pavement. The piles of a new cap foundation will also be able to absorb the horizontal actions of the diaphragm with the project maximum loads, in case of breakage (or loss of efficiency) of one or more anchors, being that no data on anchors (made in 1988) are available.

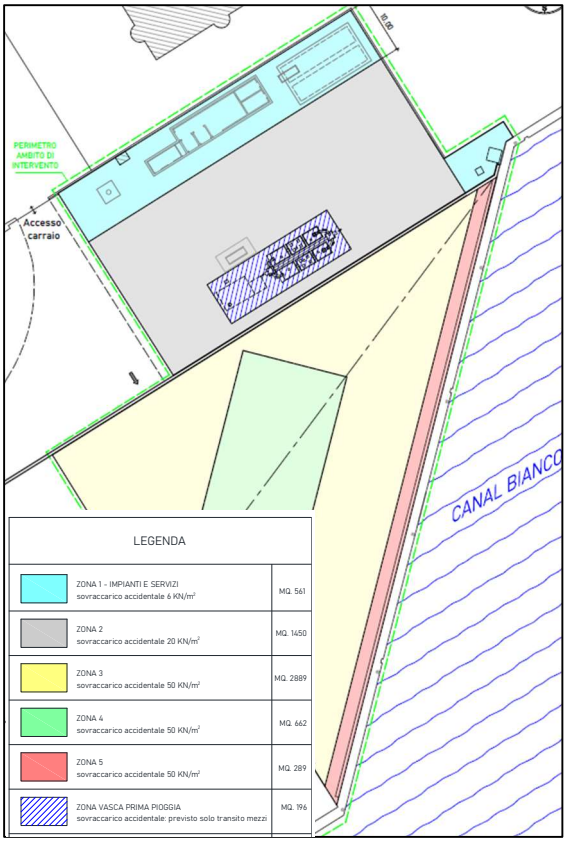

Figure 1. Subdivision of the work areas

2. Geotechnical investigation

The geotechnical investigation was carried out in 2021 and it involved the execution of two continuous core drilling at the depth of approximately 20 m, from ground level, with the withdrawal of undisturbed and disturbed samples, on which laboratory tests were carried out, 6 CPTU tests of including one with seismocone SCPTU and a DMT dilatometric test (with Marchetti flat dilatometer)

The location of the in-situ tests is shown in the following planimetry (figure 2).

Figure 2. Location of in situ tests

2.1. Stratigraphic characterization of the site

Looking at the results of in situ tests (CPTU and DMT) and continuous core drillings, the stratigraphy is highly heterogeneous.

This is clear by superimposing the Qc (tip) resistance graphs of CPTU tests, how to show in the figure 3.

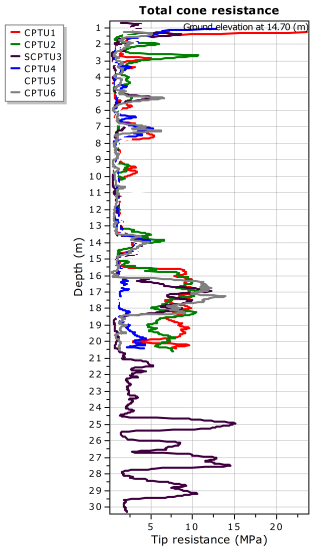

Figure 3. Superimposing CPTU

The subsoil can be roughly divided into the following stratigraphic units:

UNIT 1: it consists of landfill (at least 2÷3.3 m) of a predominantly silty and sandy nature. This is soil coming from dredging the Canal, which can be identified based on historical data. In some places there are anthropic elements such as fragments of bricks and pebbles.

• UNIT 2: a layer of predominantly silty and clayey nature with more evident peaty lenses below -8 m above ground level; however, there are layers of 0.8÷1.5 meters of sandy silt. This stratigraphic unit extends to a depth

varying between approximately -12.5 m above ground level (CPTU2) and -13.5 m (CPTU6).

• UNIT 3: sand layer which is very variable both in terms of the top and bottom depths and the thickness. In correspondence with the CPTU1 and CPTU2 tests (located to the south-west), this layer is evident and continuous, between -15 and -20 m above ground level. However, the same layer is thinner as we proceed towards the north-east, especially in zone 1.

• UNIT 4: from -20 m above ground level at -30 m above ground level (with reference to the deeper SCPTU3): there is a succession of sandy and clayey silt down to approximately -25 m above ground level, followed by silty sand with layers of sandy-clayey silt.

The geotechnical interpretations of the CPTU tests are resumed in the following tables (figure 4).

Based on CPTU tests, calibrated by the results of Laboratory Tests on undisturbed samples (classification, oedometer tests, triaxial tests) and DMT, the calculation of settlements under maximum load (20 to 50 kPa) led to very high values (up to 17 cm) and not homogeneous. Differential settlements, being very high, were deemed ineligible.

absolute sharea absolute altitude in meters above sea level: 14,3 m				CPTU1		
relative share (- m p.c.)		absolute share (m)				
from	to	from	to	description	internal friction angle (°)	cohesion (Kpa)
0	3,6	14,3	10,7	backfill soil, followed by clayey and sandy silt, water table -2,80 m p.c.	30 (up to -1,56 m p.c.)	70 (from -1,56 to -3,6 m p.c.)
3,6	5	10,7	9,3	clayey silt and silty clay, medium-low compactness		50
5	5,52	9,3	8,78	sandy clayey silt		100
5,52	6,34	8,78	7,96	clayey silt and silty clay, very low compactness		53
6,34	7,38	7,96	6,92	silty sand	35	
7,38	8,6	6,92	5,7	clayey silt sometimes sandy		73
8,6	9,66	5,7	4,64	sandy sil and silty sand	32	
9,66	13	4,64	1,3	silty clay and calyey silt sometimes sandy		71
13	14,3	1,3	0	sandy silt/silty sand	34	
14,3	15,1	0	-0,8	clayey silt		60
15,1	20	-0,8	-5,7	silty sand	35	
absolute sharea absolute altitude in meters above sea level : 14,1 m				CPTU2		
relative share (- m p.c.)		absolute share (m)				
from	to	from	to	description	internal friction angle (°)	cohesion (Kpa)
0	4,88	14,1	9,22	backfill soil, followed by sandy-clayey silt layer, soft clay froma -4 to -4,4, water table to - 2,7 m p.c.	30÷34 (sandy level)	37 (clay from -3,92 a-4,38)
4,88	8,62	9,22	5,48	silty clay and clayey silt, medium compactnes		64
8,62	9,7	5,48	4,4	clayey and sandy silt	32	
9,7	12,5	4,4	1,6	silty clay and clayey silt sometimes sandy		62,5
12,5	13,9	1,6	0,2	snady silt	34	
13,9	14,5	0,2	-0,4	clayey silt		60
14,5	20	-0,4	-5,9	silty sand	35	
absolute sharea absolute altitude in meters above sea level: 14,7 m				SCPTU3		
quote relative (- m p.c.)		quote assolute (m)				
from	to	from	to	description	internal friction angle (°)	cohesion (Kpa)
0	2,46	14,7	12,24	backfill soil and silty sand, sandy clayey silt	30 (sandy layer)	73 (da -1,62 a -2,46 m)
2,46	4,98	12,24	9,72	clayey silt /silti clay , low compactness until -3,1m , water table -3,2 m p.c.		64
4,98	9,04	9,72	5,66	succession of sandy silt (until -5,6 m), clayey silt (until -6,8m) and sandy silt	30 (fino a - 5,5)	53
9,04	13,6	5,66	1,1	silty clay and clayey silt sometimes sandy, low compactness from -9 m to -11 m		43
13,6	14,9	1,1	-0,2	silty sand and sandy silt	30	
14,9	16,1	-0,2	-1,4	clayey silt		50
16,1	18,6	-1,4	-3,9	silty sand	35	
18,6	20,5	-3,9	-5,8	silty clay transitioning to clayey silt (-19,5)		55
20,5	24,4	-5,8	-9,7	clayey and sandy silt compact	20	70
24,4	30	-9,7	-15,3	silty sand with layesr of sandy and clayey silt	35	55 (strati argillosi)

absolute sharea absolute altitude in meters above sea level: 14,3 m				CPTU4		
quote relative (- m p.c.)		quote assolute (m)				
from	to	from	to	description	internal friction angle (°)	cohesion (Kpa)
0	1,72	14,3	12,58	backfill soil and silty sand	30	
1,72	2,9	12,58	11,4	silty clay, low compactness, water table -2,80 m		54
2,9	4,08	11,4	10,22	sandy clayey silt, silty clay froma -3,4 m		54
4,08	5,6	10,22	8,7	sandy silt trasitionin (-4,6) to clayey silt	20	50
5,6	7,22	8,7	7,08	sandy silt transitioning to silty sand limo	32	
7,22	13,1	7,08	1,2	silty clay, clayey silt slightly sandy at the bottom		60
13,1	14,4	1,2	-0,1	sandy silt	30	
14,4	17,6	-0,1	-3,3	clayey silt sometimes sandy		60
17,6	20	-3,3	-5,7	sandy clayey silt transitioning to sandy silt/silty sand from -18,5 m		40
absolute sharea absolute altitude in meters above sea level: 14,5 m				CPTU5		
quote relative (- m p.c.)		quote assolute (m)				
from	to	from	to	description	internal friction angle (°)	cohesion (Kpa)
0	1,94	14,5	12,56	backfill soil an sandy silt	30	
1,94	5,76	12,56	8,74	clayey silt sometimes sandy medium compactness (less compact at approx -3,0 m) water table - 2,7 m		70
5,76	6,66	8,74	7,84	sandy silt transitioning to calyey silt		54
6,66	8,1	7,84	6,4	sandy silt and silty sand	31	
8,1	10,24	6,4	4,26	sandy and clayey silt		54
10,24	11,14	4,26	3,36	silty sand	34	
11,14	13,6	3,36	0,90	clayey silt transitioning to clayey silt (to -12,7 m)		48
13,6	14,9	0,90	-0,4	silty sand	31	
14,9	20	-0,4	-5,5	clayey and sandy silt, more sandy at the bottom from -18,5 m		60
absolute sharea absolute altitude in meters above sea level: 14,17 m				CPTU6		
quote relative (- m p.c.)		quote assolute (m)				
from	to	from	to	description	internal friction angle (°)	cohesion (Kpa)
0	5,1	14,17	9,07	backfill soil, followed from alternance of lyers of sandy silt and clayey silt, silty sand at the bottom, water table -2,8 m	30÷35 (sandy layer)	60 (clayey layer)
5,1	6,3	9,07	7,87	clayey silt (less compact at the top) transitioning to sandy clayey silt		40
6,3	6,88	7,87	7,29	silty sand	36	
6,88	8,44	7,29	5,73	silty clay/clayey silt sometimes sandy, medium compactness, sometimes low		51
8,44	13,5	5,73	0,67	silty clay/clayey silt sometimes sandy, medium compactness, sometimes low		42
13,5	14,5	0,67	-0,33	silty sand	32	
14,5	15,5	-0,33	-1,33	clayey and sandy silt		50
15,5	17,9	-1,33	-3,73	silty sand		55
17,9	20	-3,73	-5,83	sandy and clayey silt	20	50

Figure 4. Geotechnical interpretation

Zone 1:

Significant geotechnical investigations are: SCPTU3, bore hole S2 and CPTU5, from which the reference stratigraphic section is obtained (figure 5).

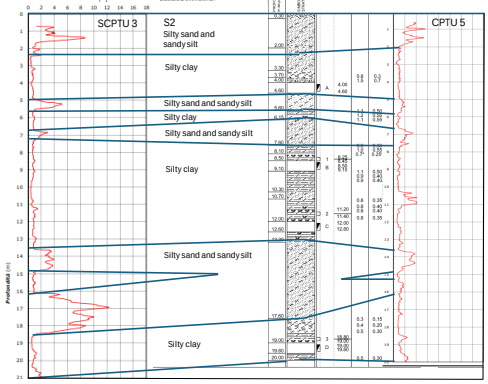

Figure 5. Stratigraphic section zone 1

In this area, four load-bearing piles, vibro-driven (without removal of soil) 15 meters long, were built, above which the plinth will be cast to support the light tower.

Furthermore, 24 settlement reducing piles were constructed (pile length 6.5 m) above which the foundation slab of the C01 electrical substation will be cast.

Zone 2:

The stratigraphy in this area is represented by the tests CPTU2, CPTU6 and the bore hole S2, below (figure 6) is shown the stratigraphic section, which confirms the extreme variability.

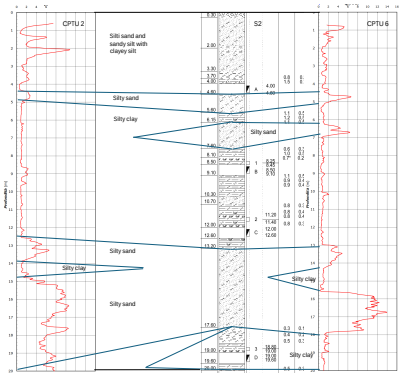

Figure 6. Stratigraphic section zone 2

In this zone were installed piles 8 m long, with spacing of 3.60 m, distributed over the whole area, always with the aim of reducing settlements.

Zone 3:

In this case the piles were always installed at a depth of -8 m with spacing 2.5 m, with the aim of reducing the expected settlement.

3. Type of pile

As regards the type of pile, the solution was chosen to create piles with a diameter of 35 cm without removing the soil (with a steel casing vibrated down to the final depth) and cast on site with reinforced concrete.

For simplicity, depending on the design loads, the length, spacing and reinforcement were varied without changing the type of pile, diameter and structure of the foundation slab (except for zones 4 and 5, where structures are different from those of the zones 2 and 3).

The distribution of the piles in planimetry is as shown below.

The project piles are built according to the following phases:

- Driving a casing with a diameter 350 mm equipped with a valve in the bottom, by means of vibration (vibrated piles) or rotation (roto-driven piles);
- Installation of the reinforcement;
- Insertion of the hopper at the bottom of the hole and casting of concrete of suitable characteristics, possibly with additives;
- Extraction of the casing (always vibrating or rotating the casing)) and simultaneous saturation of the hole with concrete.

These piles allow for significant soil compaction and at the same time the absence of soil to be removed.

Figure 7 shows the location of the poles in plan.

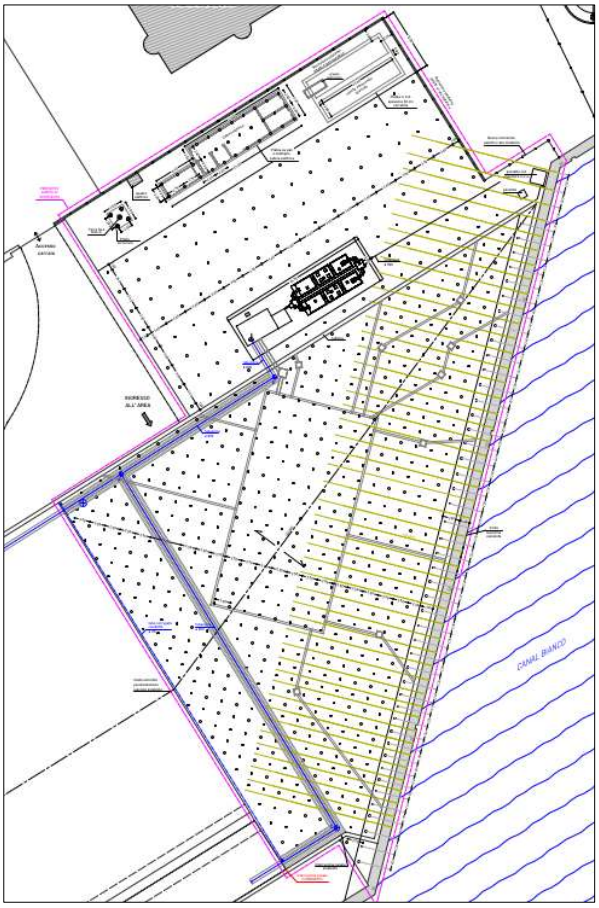

Figure 7. Plan with location of the piles

4. HVSR single station measurement (H/V):

4.1. Procedure and instrumentation used.

The HVSR (Horizontal to Vertical Spectral Ratio) method proposed by Nagoshi and Igarashi (1970) and subsequently modified by Nakamura (1989), is based on the analysis of the spectral ratio between the horizontal (H) and vertical (V) components of the seismic noise registered on a site. Seismic noise is present everywhere and is generated both by atmospheric phenomena (ocean waves, wind) and by human activity. Seismic noise is often referred to as microtremor since it is characterized by very weak oscillations (of the order of μm/s). Microtremors are partly made up of volume waves, P or S, but above all by surface waves, the speed of which is however close to that of S waves (Mulargia et al., 2007). The seismic noise measurement technique requires recording times of 15-20 minutes and requires three-way seismology sensors with levelling, a 24-bit digitizer with high dynamics, high gain and high native sampling frequency, with minimization of electromagnetic and mechanical noises.

The acquisition was performed using a GEOBOX SR04 digital seismograph equipped with 3 velocity sensors with a nominal frequency of 2Hz (N-S, E-W, Up-Down) and a 24bit digitizer for the acquisition of the

microtremor. The seismograph also has built-in GPS for synchronization.

In the case in question, several stations were carried out, before (an example in figure 8) and after (an example in figure 9) the piling intervention, to measure the seismic noise for a recording time of 20 minutes each. The processing of the acquired seismic noise data took place using the SISMOWIN software from SARA electronics srl and the GEOPSY software developed within the SESAME research program funded by the European community. The inversion of the eliptical curve obtained with Geopsy/Sismowin occurred via the Dinver component of the same Geopsy software. To perform the inversion of the eliptical curve, reference was made to the geotechnical investigations (SCPTU, CPTU and surveys) carried out on the area. Using the Geopsy "Dinver" software it was possible to define the seismographic model of the subsoil and perform an estimate of the Vs30 speeds.

The location of the stations is shown in figure 10.

Figure 8. (HVSR3) Tests before the construction of the piles

Figure 9. (HVSR3) tests after the construction of the piles

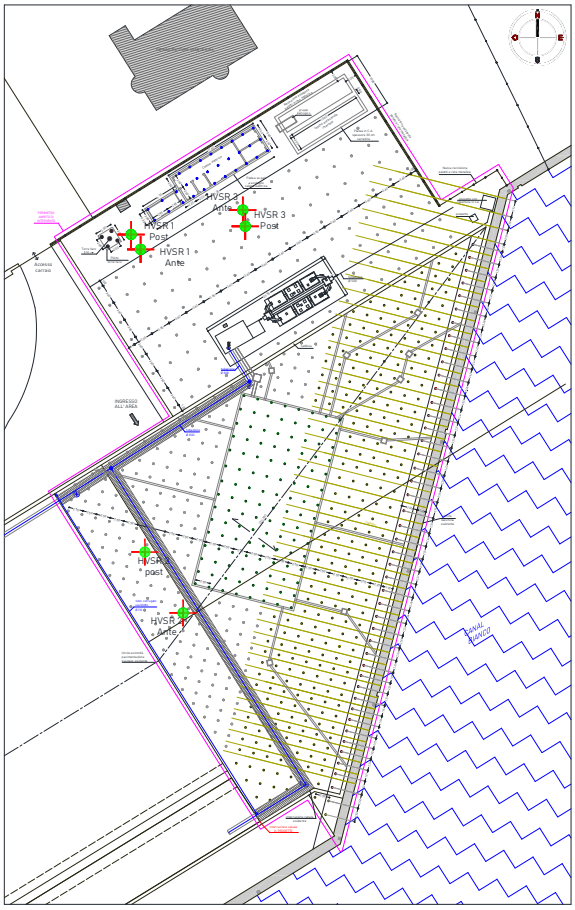

Figure 10. Location of the tests

5. Results and data analysis relating to seismic noise acquisition

5.1. H/V spectral ratio curves and seismostratigraphic model

In the various tests, the acquisition of seismic noise was carried out for a recording time of approximately 20 minutes with a sampling frequency of 300. The processing of the acquired data carried out using Geopsy software gave rise to the curves of the spectral ratios H/V above.

The H/V curve relating to a multi-layer system contains information relating to the resonant frequency (and therefore the thickness) of each of them.

In the figures shown in the following paragraphs, the solid black curve represents the average H/V ratio, while the dashed black curves, called "confidence curves", are the result of the multiplication (upper curve) and division (lower curve) of the H/V ratio average values for the standard deviation of the values of the individual H/V curves. The two grey bands identify the main frequency, or f0, automatically identified by the program. The f0 of the average ratio is exactly in the centre of the two bands, while the area covered by the bands is obtained by adding and subtracting the standard deviation of the f0 of the individual curves from the f0 of the average ratio.

For each test are shown on the graphs below, the significative results.

5.2. Test HVSR1 carried out before and after the construction of the piles.

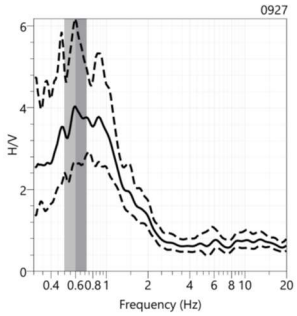

Figure 11. Curves H/V – HVSR1 - before the construction of the piles

Figure 11 shows the H/V spectral ratio curve referring to the HVSR1 station before the construction of the piles. The peak is highlighted the peak is highlighted at the contact between the two grey bands, the standard deviations are highlighted with the dotted line.

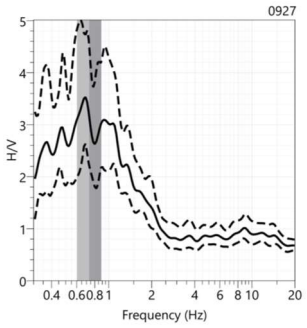

Figure 12. Curves H/V – HVSR1 - after the construction of the piles.

Figure 12 shows the H/V spectral ratio curve referring to the HVSR1 station after the construction of the piles. The peak is highlighted at the contact between the two gray bands, the standard deviations are highlighted with the dotted line.

Figure 13 shows the HSVR1 earthquake comparing, after the construction of the piles, as a function of deph and respectively of Vp and Vs speeds

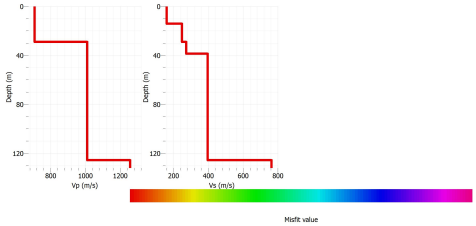

Figure 13. HVSR1 earthquake model after the construction of the piles.

Below (figure 14) are the graphs (H/V-frequency) comparing the experimental curves before and after the construction of the piles. The second graph shows the values with frequencies up to 4 Hz, in order to highlight the first section of the curves.

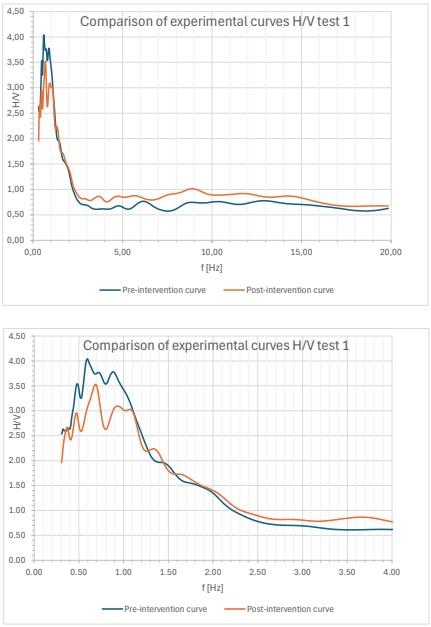

Figure 14. HVSR1 – comparison of experimental curves

5.3. Test HVSR2 carried out before and after the construction of the piles.

This paragraph shows the same graphs seen previously but referring to the HSVR2 test.

Figure 15 shows the H/V spectral ratio curve referring to the HVSR2 station before the construction of the piles.

.

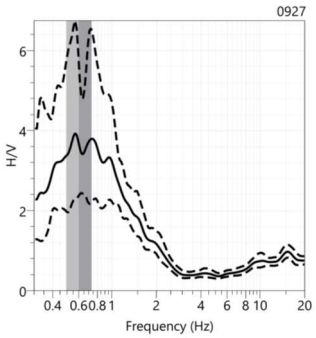

Figure 15. Curves H/V – HVSR2 - before the construction of the piles

Figure 16 shows the H/V spectral ratio curve referring to the HVSR2 station after the construction of the piles.

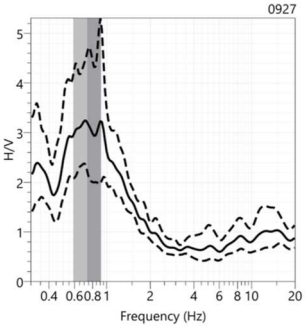

Figure 16. Curves H/V – HVSR2 - after the construction of the piles

Figure 17 shows the HSVR1 earthquake comparing, after the construction of the piles, as a function of deph and respectively of Vp and Vs speeds.

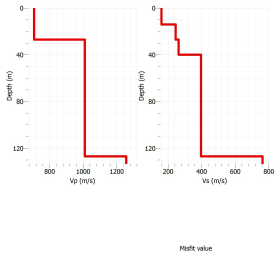

Figure 17. HVSR2 earthquake model after the construction of the piles, as a function of depth and respectively of Vp and Vs speeds

Below (figure 18) are the graphs (H/V-frequency) comparing the experimental curves before and after the construction of the piles. The second graph shows the values with frequencies up to 4 Hz, in order to highlight the first section of the curves.

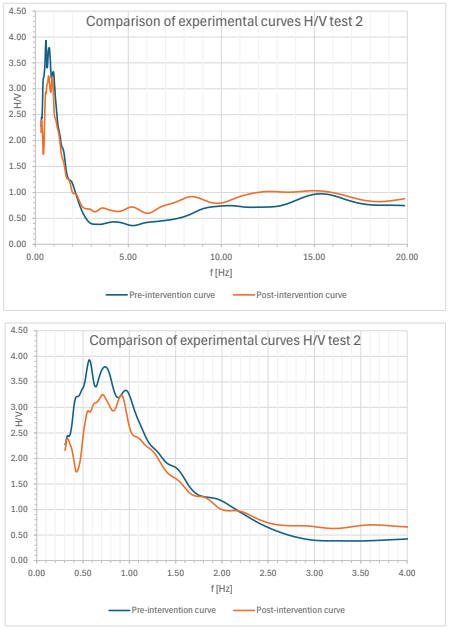

Figure 18. HVSR2 – comparison of experimental curves.

5.4. Test HVSR3 carried out before and after the construction of the piles.

This paragraph shows the same graphs seen previously but referring to the HSVR3 test.

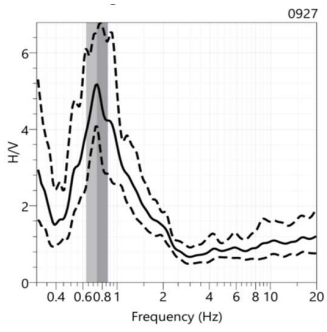

Figure 19. Curves H/V – HVSR3 - before the construction of the piles

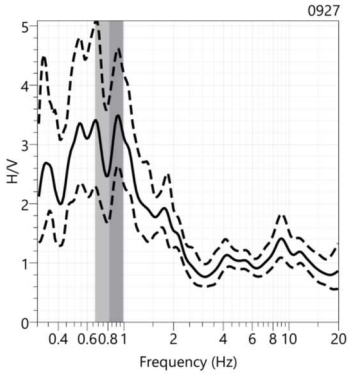

Figure 20. Curves H/V – HVSR3 - after the construction of the piles

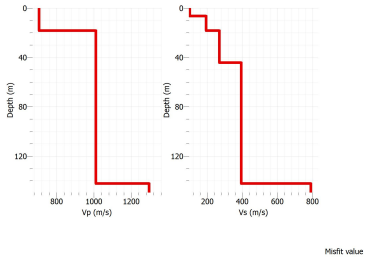

Figure 21. HVSR3 earthquake model after the construction of the piles, as a function of depth and respectively of Vp and Vs speeds

Below are the graphs (H/V-frequency) comparing the experimental curves before and after the construction of the piles. The second graph shows the values with frequencies up to 4 Hz, to highlight the first section of the curves.

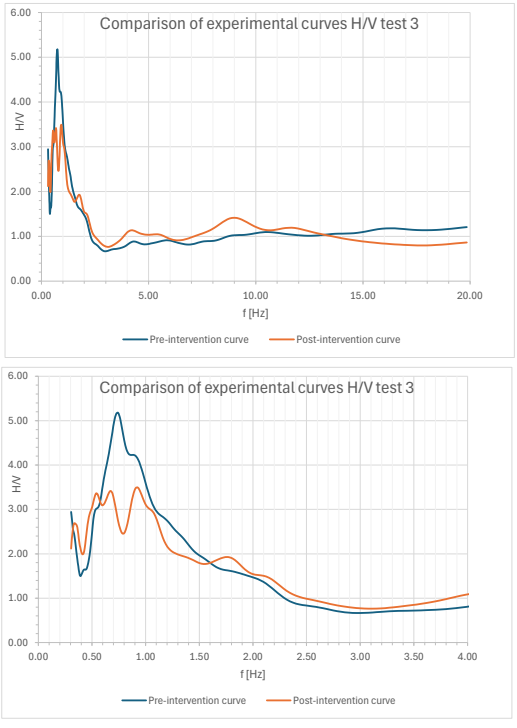

Figure 22. HVSR3 – comparison of experimental curves.

6. Conclusions

On this site the available geological information allows the deposit to be considered as horizontally layered with a smooth and flat interface with the underlying bedrock.

Generally, low frequency H/V peaks are associated either with extremely soft soil with a thickness of several tens of meters, or with "normal" soil deposits having a very large thickness (several hundred meters at least): the former case is obviously associated with a large impedance contrast, while this can occur in the latter case only if the bedrock is very hard. Indeed, in all the tests we have a low frequency H/V peaks (< 1 Hz) more o less clear.

The main information looked for within the H/V ratio is the fundamental natural frequency of the deposits, corresponding to the peak of the H/V curve. While the reliability of its value will increase with the sharpness of the H/V peak, no straightforward information can be directly linked to the H/V peak amplitude A0. This latter value may however be considered as indicative of the impedance contrasts at the site under study: large H/V peak values are generally associated with sharp velocity contrasts.

Generally, the comparison between the H/V ratio of ambient vibrations and the standard spectral ratio of earthquakes using a reference site, shows that it is not scientifically justified to use A0 as the actual site amplification. However, there is a general trend for the H/V peak amplitude to underestimate the actual site amplification. In other words, the H/V peak amplitude could generally be considered as a lower bound of the actual site amplification. In all tests is show that the peak amplitude A0 decreases due to consolidation with concrete piles, and this suggests a minor seismic amplification.

Comparison peak amplitude A_0

	A_0 Pre-intervention	A_0 Post-intervention
Test 1	4.04	3.53
Test 2	3.93	3.25
Test 3	5.18	3.42

Comparison peak frequency

	Pre-intervention Peak Frequency [Hz]	Post-intervention Peak Frequency [Hz]
Test 1	0.6	0.73
Test 2	0.6	0.73
Test 3	0.74	0.81

As is known, the classification of the subsoil is carried out based on the stratigraphic conditions and the values of the equivalent velocity of propagation of the shear waves, $V_{S,eq}$ (in m/s), defined by the expression:

$$V_{S,eq} = \frac{H}{\sum_{i=1}^{N} \frac{h_i}{V_{S,i}}}$$

The inversion of the H/V curve allows the values of the Vs shear waves to be estimated. From the comparison between the values before and after the intervention, a slight increase in the equivalent value can be observed of shear waves, $V_{S,30}$ (in m/s).

Comparison $V_{s,30}$

	Pre-intervention $V_{s,30}$ [m/s]	Post-intervention $V_{s,30}$ [m/s]
Test 1	189	199
Test 2	190	199
Test 3	172	180

Based on the results obtained, will be useful to deepen the study, analysing (for the same type of pile i.e. vibro or roto-driven piles) the variation of the V_{s30}, as a function of the distance between the centres of the piles, their diameter, as well as the depth, which, in the analysis performed, is still modest.
Since further projects are planned in the same area, it will be possible to proceed with an in-depth analysis of this study.

Acknowledgements

Authors wish to thank INFRASTRUTTURE VENETE and INTERPORTO DI ROVIGO spa for letting use the data.

References

Guidelines for the implementation of the h/v spectral ratio technique on ambient vibrations".

SESAME: Site Effects assessment using Ambient Excitations.
European Commission, contract n° EVG1-CT-2000-00026.